한국박용기관학회지 제27권, 제5호, pp. 590~599, 2003 (ISSN 1226-9549)
Journal of the Korean Society of Marine Engineers

초음파 진동을 이용한 마찰 및 음향부상에 의한 물체의 수송

박 용 국† · 노 병 국*

(원고접수일 : 2003년 2월 21일, 심사완료일 : 2003년 5월 9일)

Friction-Based and Acoustically-Levitated Object Transport Using Ultrasonic Vibration

Yong-Kuk Park† · Byoung-Gook Loh*

Key words : Ultrasonics (초음파), Traveling waves (수송파), Acoustic levitation (음향부상), Frictional drive (마찰 구동), Piezoelectric actuator (압전모터)

Abstract

In this study, object transport method based on ultrasonic flexural vibration is presented. Ultrasonic vibration generates ultrasonic traveling waves on the surface of elastic medium. Objects are transported through the interaction with traveling waves propagating in medium. Two types of transport methods are studied: frictional drive and acoustic levitation. With frictional drive, objects are transported in contact with the beam in the opposite direction of wave propagation whereas with acoustic levitation, objects are acoustically levitated above the beam surface and transported in the wave propagation direction. Transport characteristics are experimentally investigated using objects of different shapes and sizes. The transition from acoustic levitation mode to frictional drive mode is also examined, and it is found to occur when the ratio of mass to area of an object exceeds the threshold ratio of mass to area. It is envisaged that this feasibility study will serve as a stepping-stone for ultrasonic vibration to become an effective industrial material handling device in the future.

1. Introduction

Methods of transporting objects using ultrasonic flexural vibrations are based on the generation of ultrasonic traveling waves on the surface of elastic medium [1-3]. As traveling waves propagate on the surface of elastic medium, particles on the surface move in an elliptic path [4-6]. Relatively heavy objects come in contact

† 책임저자(대구가톨릭대학교 기계자동차공학부) E-mail : ykpark@cu.ac.kr, T : 053)850-2723
* 대구가톨릭대학교 기계자동차공학부

with medium, and are driven in the opposite direction of wave propagation due to frictional force. Light objects with planar surface are levitated above medium by acoustic levitation pressure, and transported in the direction of wave propagation.

Advantages of such a system involve absence of a magnetic field, silent operation, and the use of a simple structure. The presence of magnetic fields generated by electromagnetic motors is detrimental to many industrial environments including semiconductor manufacturing, and magnetic resonance imaging. Therefore, an object transport system in the absence of a magnetic field would be quite useful in these environments. Quiet operation is achieved by ultrasonic excitation which is not detected by human ears. The simple structure due to lack of moving parts including conveyor belts, gears, and bearings enables maintenance issues minimal.

Most of the previous works on using ultrasonic vibrations as driving source have been confined to ultrasonic motors [7]. Not much research has considered ultrasonic vibration as source for a transporting mechanism. Ro et al. investigated feasibility of using ultrasonic flexural vibrations as a material handling mechanism [2]. Hashimoto et al., and Hu et al. studied acoustic levitation as a non-contact transport mechanism [8, 9]. Previous research on the object transport studied frictional drive and acoustic levitation as a separate matter of subject, except where feasibility of using frictional drive and acoustic levitation as a transport mechanism was briefly introduced along with its transition characteristics [2]. In fact, two modes of operation, frictional drive and acoustic levitation co-exist and are closely related. Hence, it is imperative to understand working principles and characteristics of respective mode of operation to make the most of this promising technology as transport mechanism. Moreover, a mode transition, that is, change of driving force from friction to acoustic levitation or vice versa, is one of the important characteristics of the transport mechanism using ultrasonic vibration. Ensuing research is needed to have full understanding of it because the transport system would not be put to practical use unless the transport direction is known in advance. Therefore, the objective of this study is to investigate the nature of each mode of operation and its transition characteristics.

2. Construction of a Prototype

Fig. 1 shows the prototype is comprised of a beam and modules that contain piezoelectric actuators and horns. It is also illustrated in Fig. 2. The modules function in either an active or passive manner. The active module excites flexural vibrations on one end of the beam while the passive module absorbs the vibrations through impedance matching. Impedance matching is a process of dissipating the energy transported by wave propagation by proper selection of a resistor and inductor to match the impedance of the system [2]. Accordingly, waves excited from the one end of the system are dissipated at the other end and the reflection of the waves is prevented, thereby generating traveling wave.

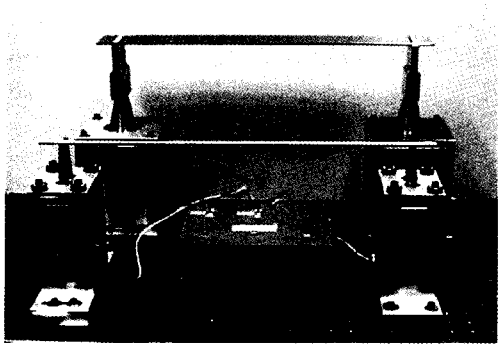

Fig. 1 General view of prototype.

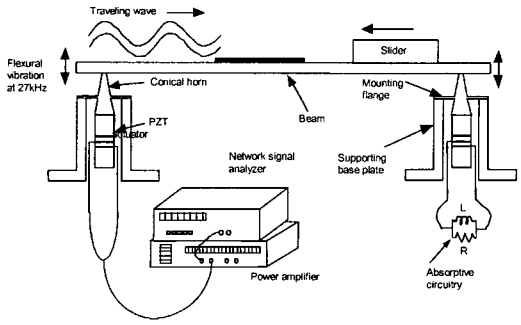

Fig. 2 Schematic drawing of the prototype.

A beam and horns are made of aluminum (6061-T6) because of the excellent acoustical characteristics of this material. The size of the beam is 11 mm wide, 3.1 mm thick, and 500mm long. The piezoelectric actuators are bolted Langevin type transducers manufactured by NGK Spark Plug Co. Ltd. (model no. DA2228). Their resonant frequency is 28 kHz. The conical horns are employed to amplify the amplitude of vibration of the actuators, maximizing the displacement of the beam for a given power supply. A conical geometry is chosen because it not only gives a desired amplification ratio but also can be easily machined. The location of nodal lines and dimensions of conical horns are determined following the procedures detailed by Merkulov [10]. An amplification ratio of 3.75 is selected for the prototype. A mounting flange is included in the design of the horn, and is located at the nodal lines where the velocity of vibration of the horn goes to zero. This configuration allows the mounting of the horn and actuator assembly onto a supporting base plate that is in turn bolted to an air-vibration-absorption table surface.

When fully assembled, the assembled structure is sine-swept using a Stanford Research Systems model SR780 network signal analyzer to find the excitation frequency that gives the maximum vibration displacement of the beam. The measured frequency is 27.15 kHz. Sine wave voltage synthesized by network signal analyzer is amplified using a Trek model 50/750 power amplifier before being supplied to the active module at one end of the beam. A control box shown in Fig. 1 enables manual switching of the direction of the traveling waves by connecting either the excitation sine wave voltage or absorptive circuitry to either active or passive module.

3. Working Principles

3.1 Generation of Traveling Wave

Traveling waves can be generated through the use of a passive absorbing module connected to one end of the beam. The impedance of the absorptive module should be made equal to the characteristic impedance of the transmission beam and the piezoelectric actuator through

impedance matching. Impedance matching is achieved by connecting an electrical circuit in which a resistor and an inductor are connected in parallel to the actuator on the passive end. The resistance and inductance values were determined using transmission line theory [4]. Minimizing the presence of any standing waves is crucial to the performance of the system. The generation of standing waves created by poor component connection must be avoided. Therefore, the components are bonded together with cold-hardened epoxy to ensure perfect contact between the actuators, horns, and beam.

3.2 Object Transport Using Frictional Drive

When traveling waves are generated through a beam, particles on the surface of the vibrating beam move elliptically. An object on the beam is forced to move toward the excitation source through frictional force if the object has non-flat surface or its ratio of mass to area is greater than a certain threshold value. The threshold value is discussed in Section 4.3. This concept is illustrated in Fig. 3.

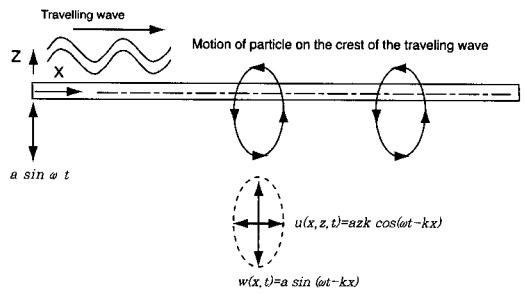

Fig. 3 Principle of elliptic motion (See definitions in Equation (1)-(5)).

The governing equation of a vibrating beam is

$$\frac{\partial^4 w}{\partial x^4} + \frac{\rho A}{EI}\frac{\partial^2 w}{\partial t^2} = 0 \tag{1}$$

where,

w : displacement in the z-direction

ρ : mass density of the beam,

A : cross sectional area,

E : Youngs modulus,

I : moment of inertia

The solution of the above equation is

$$w(x,t) = a\sin(\omega t - kx) \tag{2}$$

where,

a : vibration amplitude,

ω : periodic frequency of the flexural waves

The wave number k is defined as

$$k = 2\pi/\lambda = \omega^{1/2}(\rho A/EI)^{1/4} \tag{3}$$

The longitudinal displacement $u(x,z,t)$ depends on the thickness of the beam in the z-direction; that is, the distance from the neutral axis of the beam. As this distance gets larger, the horizontal motion due to bending of the beam is greater. This displacement can be written as:

$$u(x,z,t) = -z\frac{\partial w}{\partial x} = azk\cos(\omega t - kx) \tag{4}$$

$$\frac{u^2}{(azk)^2} + \frac{w^2}{a^2} = 1 \tag{5}$$

which is clearly an elliptic path as shown in Fig. 3.

As the motion of a particle on the beam surface reaches the extent of its vertical

travel, the component of velocity in the direction tangent to the beam is at maximum. Equation (6) describes the maximum velocity of a particle at the surface of the beam and consequently the maximum possible velocity of any object on the beam.

$$V_u = \frac{\partial u}{\partial t} = -a\frac{h}{2}k\omega \sin(\omega t - kx) \quad (6)$$

where,

h : thickness of beam

Vu : longitudinal velocity

If the mass of an object on the beam is not large enough to significantly deform the beam, contact between the object and the beam is likely to occur only at the crest of wave as shown in Fig. 4.

When the traveling waves pass under the slider, it is driven by the friction force $F\mu$ which is defined as:

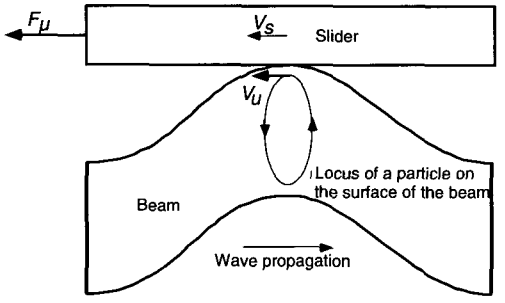

Fig. 4 Dynamic model of beam and slider interaction (See definitions in Equation (7)).

$$F_\mu = \mathrm{sgn}(V_u - V_s)\mu mg \quad (7)$$

where,

Vs : velocity of slider

Vu : peak longitudinal velocity

μ : frictional coefficient between beam and slider

g : gravitational acceleration (9.8m/s2)

m : mass of slider

sgn: signum function defined as

sgn(x) = 1 if x>0

-1 otherwise

The direction of friction force $F\mu$ is determined by the relative velocity between Vs and Vu. Setting friction force equal to inertia force gives

$$\dot{V}_s = \mathrm{sgn}(V_u - V_s)\mu g \quad (8)$$

Provided that there is no sliding between the object and the beam, the speed of the object theoretically equals the longitudinal velocity at the crest of the wave, which is shown in equation (8). As the mass of the object increases, contact takes place over a larger area. The speed of the object equals the average longitudinal vibration velocity of the contact area. Longitudinal vibration velocity is maximum at the crest of the wave and decreases sinusoidally beyond the crest of the wave as shown in equation (6). As a result, the speed of the object is inversely proportional to the mass of the object.

3.3 Object Transport Using Fluid Coupled Acoustic Levitation

Acoustic waves propagate from a flexurally vibrating beam as shown in Fig. 5. If a planar object is placed on the beam, the object acts as a reflector of the propagating acoustic waves. The object is levitated due to the acoustic radiation pressure. Using linear acoustic theory, the levitation distance has been described by equation (9).

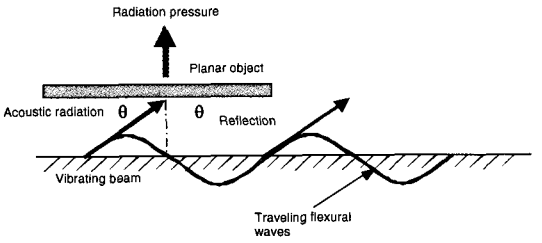

Fig. 5 Acoustic levitation.

$$H = Ca\sqrt{\frac{\rho}{2W}} \tag{9}$$

where,

H : levitation distance
C : sound velocity in air
a : peak vibration amplitude of beam
ρ : density of air
W : weight/area of planar object

Describing the forces that act upon the object to transport it along the beam is done from a fluid mechanics perspective. There is an air velocity gradient that exists near the surface of the beam that travels along the beam's length as shown in Fig. 6. This air flow effectively propels light, flat objects along the length of the beam in the direction of wave propagation due to the fluid shear forces [9]. A governing equation that describes this air velocity gradient and the effect on the transport speed of an object has not been developed.

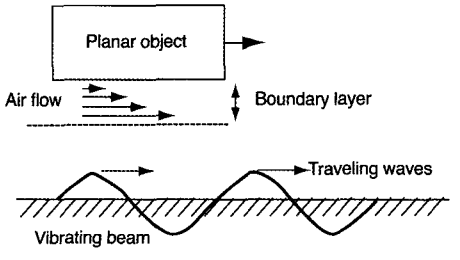

Fig. 6 Acoustic transportation

4. Experimental Results

4.1 Frictional Drive

Measurements of the beam vibration amplitude are taken using a photonic sensor as a function of input voltage. A plot of the beam vibration amplitude versus input voltage is shown in Fig. 7. The vibration amplitude of the beam is linearly proportional to the input voltage. Various sliders are made to investigate the object transporting capabilities of ultrasonic vibration. The sliders are constructed using aluminum and steel of varying lengths, thereby varying the contact area between the slider and beam. The contact surface presented to the beam is made flat and relatively smooth. Various other objects including coins and integrated circuit (IC) chips are also employed to determine experimentally the optimum characteristics producing the maximum transportation speed.

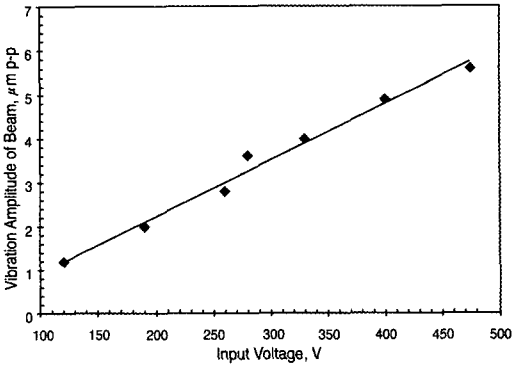

Fig. 7 Beam vibration amplitude vs. input voltage.

Experiments are performed with input voltage of 330 V, excitation frequency of 27 kHz, and peak beam vibration amplitude of 2 μm. The displacements of various

sliders obtained from frictional drive are measured using an infrared sensor and the results are shown in Fig. 8. The average velocities are estimated from the slope of the displacement versus time plot. The results are shown in Fig. 9 and Fig. 10. The sliders with a contact area of 132 , 240, 504 and 693 mm2 are made of steel with a mass of 18, 40, 85, and 96 g, respectively. Results indicate that transport velocity increases as contact area and mass decrease. Results agree well with the theoretical prediction that a maximum velocity is achieved when the contact between the object and medium occurs at the crest of a wave as shown in equation 6. As weight of an object increases and contact area increases, it results in decrease in transport speed. Other objects are also examined to investigate the effect of changing size, shape, surface finish, coefficient of friction, and mass on the speed of the object along the beam. Results are shown in Fig. 11. Measured velocity of a nickel is 7.9 cm/s, 8.2 cm/s for a capacitor, and 5.2 cm/s for a large block of steel.

cm/s for a large block of steel.

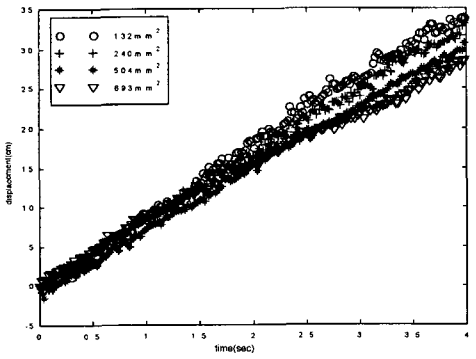

Fig. 8 Displacement - frictional drive.

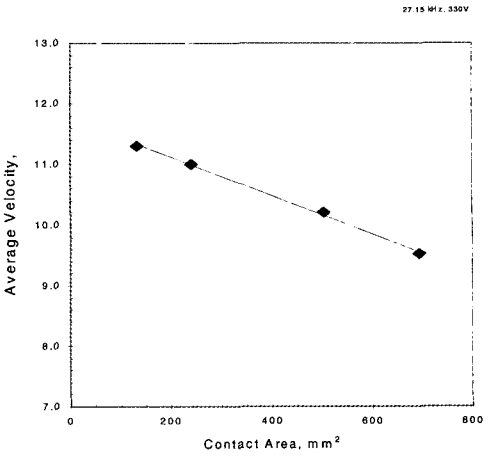

Fig. 9 Contact area vs. average velocity - frictional drive.

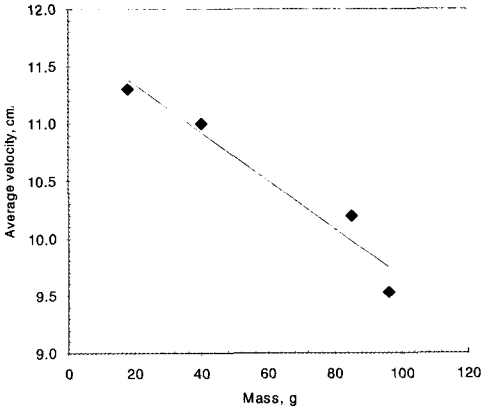

Fig. 10 Mass vs. average velocity - frictional drive.

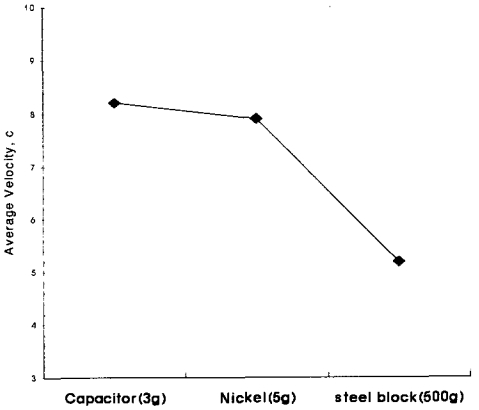

Fig. 11 Average velocity of objects of different shape - frictional drive.

4.2 Acoustic Levitation

The transport speeds of objects supported by an air film and driven through acoustic levitation are also measured using three different IC chips. Applying a load to the beam causes the beam to undergo flexure. The maximum flexure at the center of the beam is approximately 1 mm. Since there is no contact between the vibrating beam and the IC chips, the slope of the beam had an effect on the transport velocity. To gage the effect of the beam slope on the chip velocity, testing is performed. An IC chip is placed at the center of the beam, i.e., at the point of maximum deflection, and allowed to levitate. The IC chip goes up the slope and reaches the end of beam with mild decrease in velocity. The test result shown in Fig. 12 is initiated from the end of the beam. This test is done to find the greatest possible transport velocity for a given IC chip. However, the transport velocity is observed to increase over time. The saturation of transport speeds is not observed given the length of the beam.

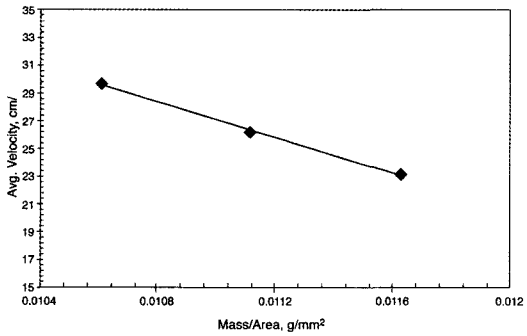

Fig. 12 Mass/area vs. average velocity-acoustic levitation.

4.3 Transition from Acoustic Levitation to Frictional Drive

When light flat-surfaced sliders are placed on the surface of the beam, a "floating" phenomenon, objects simply floating above the beam but not moving, occurs. The floating behavior is that neither frictional drive nor transport by acoustic levitation occurs. The cause of this behavior is the ratio of weight to area of the object in the range of making the acoustic levitation arise but the generated shear force tangent to the beam surface is not great enough to overcome its own inertia. Of great importance is the transition range where the capability of frictional drive is completely offset by acoustic levitation. As stated earlier, transport direction by friction mode is opposite of acoustic levitation mode. Therefore, within a critical region that involves the area of a flat slider surface and its weight, the mode transition can occur. An experiment shows that for some range, a slider locally swings back and forth, indicating obvious transition. Sliders of different lengths are constructed to modify the surface area in contact with the beam. The sliders are also designed to accommodate the stacking of weights on top in order to vary the mass and consequently the normal and frictional forces.

Tests are conducted to experimentally determine the point at which frictional drive overcome the floating due to acoustic levitation. The experimental results shown in Fig. 13 appear to indicate that at slider lengths below one wavelength (3 cm), there is an increased

capacity to levitate mass with an increase in slider length. At slider lengths near one wavelength, the capabilities of acoustic levitation drop off significantly. At slider lengths beyond one wavelength, the levitation capability recovers.

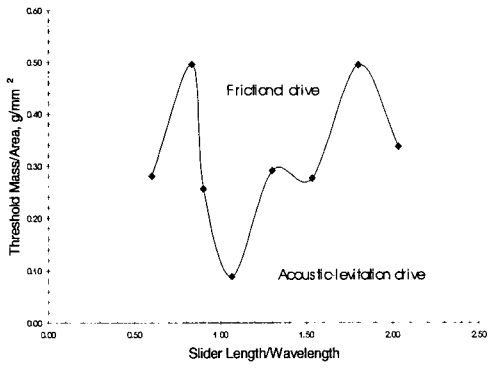

Fig. 13 Transition of driving force.

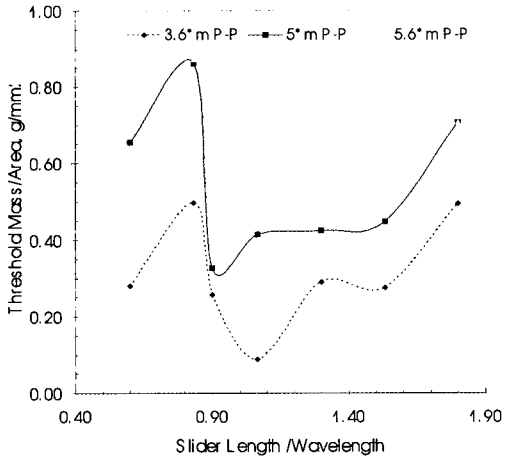

Fig. 14 Transition from acoustic to frictional drive.

When a certain size slider is placed on the vibrating beam, three things can occur: transport by friction; transport by acoustic levitation; or float (stationary) depending on its mass to area ratio. At the ratio of mass for area above the curve in Fig. 13, the slider will be driven by friction force. Below the curve, acoustic levitation will be the driving force. In the vicinity of the curve the slider will float. Therefore, this region must be avoided for implementation. Fig. 14 exhibits transition of driving forces for three different vibration amplitudes of beam (3.6, 5, and 5.6μm).

5. Conclusions

Ultrasonic vibration as a transport mechanism has been investigated theoretically and experimentally. Object transport speeds of 11 cm/s using friction mode and 30 cm/s using acoustic levitation mode with a power input of 20 W are obtained for a wave propagation velocity of 800 m/s. With these transport speeds, the demands of manufacturing industries can be effectively matched.

The threshold mass to area ratio causing mode transition is also experimentally identified. This threshold ratio increases as the slider length approaches the wavelength. It decreases at slider length near the wavelength. At slider length beyond the wavelength, it increases again.

Limitation of transport using acoustic levitation is that only light and planar objects can be transported. In addition to faster transport speed, however, the advantage of this non-contact transport mechanism would make transport by acoustic levitation ideal for clean-room based manufacturing environment, such as semi-conductor manufacturing industry.

Acknowlegements

This research work was supported by the 2003 research grant of Catholic University of Daegu.

References

[1] W. C. Elmore, Physics of Waves, McGraw-Hill, pp. 5-13, 1969.

[2] P. I. Ro, B-G. Loh, J. Santiago, Feasibility of Contact and Noncontact Material Handling Using Traveling Waves and Transition Characteristics, IEEE Transactions on Industrial Electronics, Vol. 47, No.6, pp. 1344-1345, 2000.

[3] B. G. Loh, and P. I. Ro, An Object Transport System Using Flexural Ultrasonic Progressive Waves Generated by Two-Mode Excitation, IEEE transactions on ultrasonic, ferroelectrics, and frequency control, pp. 994-999, 2000.

[4] M. Kuribayashi, S. Ueha, E. Mori, Excitation Conditions for Flexural Traveling Waves for a Reversible Ultrasonic Linear Motor, Journal of Acoustical Society of America, Vol. 77(4), pp. 1431-1435, 1989.

[5] M. Kurasawa, S. Ueha, High Speed Ultrasonic Linear Motor with High Transmission Efficiency, Ultrasonics, Vol. 27, January, pp. 39-44, 1989.

[6] Y. Tomikawa, K. Adachi, H. Hirata, T. Suzuki, and T. Takano, Excitation of Progressive Wave in a Flexurally Vibrating Transmission Medium, Proceedings of 10th Symposium on Ultrasonic Electronics, Vol. 29-1, pp. 179-181, 1989.

[7] T. Sashida, An Introduction to Ultrasonic Motors, Clarendon Press, Oxford, 1993.

[8] Y. Hashimoto, Y. Koike, and S. Ueha, Acoustic Levitation of planar objects using a longitudinal vibration mode, J. Acoust. Soc. Jpn. (E)16, Vol. 3, pp. 189-192, 1995.

[9] J. H. Hu, K. Nakamura, and S. Ueha, Characteristics of a Non-contact Ultrasonic Motor Using Acoustic Levitation, IEEE Ultrasonic Symposium, pp. 373-376, 1996.

[10] L. G. Merkulov, Design of Ultrasonic Concentrators, Sov. Phy.-Acoust., Vol. 3, pp. 246-255, 1957.

저 자 소 개

노병국 (盧炳國)

1969년 2월생. 1993년 고려대학교 기계공학과 졸업. 1995. North Carolina State University(공학석사). 1996-1997 (주)포스코개발. 2000년 North Carolina State University(공학박사). 2001-2002 IBM Data Storage Division(USA) 2002-현재 대구가톨릭대학교 기계자동차공학부 전임강사

박용국 (朴鏞國)

1964년 11월생. 1987년 서울대학교 공학사. 1989년 University of Michigan(공학석사). 1995. Ohio State University(공학박사). 1996. Ohio State University (Post-Doctoral). 1996-1998년 삼성자동차 금형기술연구소. 1998-현재 대구가톨릭대학교 기계자동차공학부 조교수.